



## Doping asymmetry of superconductivity coexisting with antiferromagnetism in spin fluctuation theory

Rowe, W.; Eremin, I.; Romer, A. T.; Andersen, B. M.; Hirschfeld, P. J.

*Published in:*  
New Journal of Physics

*DOI:*  
[10.1088/1367-2630/17/2/023022](https://doi.org/10.1088/1367-2630/17/2/023022)

*Publication date:*  
2015

*Document version*  
Publisher's PDF, also known as Version of record

*Citation for published version (APA):*  
Rowe, W., Eremin, I., Romer, A. T., Andersen, B. M., & Hirschfeld, P. J. (2015). Doping asymmetry of superconductivity coexisting with antiferromagnetism in spin fluctuation theory. *New Journal of Physics*, 17, [023022]. <https://doi.org/10.1088/1367-2630/17/2/023022>

## Doping asymmetry of superconductivity coexisting with antiferromagnetism in spin fluctuation theory

This content has been downloaded from IOPscience. Please scroll down to see the full text.

2015 New J. Phys. 17 023022

(<http://iopscience.iop.org/1367-2630/17/2/023022>)

View [the table of contents for this issue](#), or go to the [journal homepage](#) for more

Download details:

IP Address: 130.225.212.4

This content was downloaded on 24/05/2016 at 07:59

Please note that [terms and conditions apply](#).



## PAPER

## Doping asymmetry of superconductivity coexisting with antiferromagnetism in spin fluctuation theory

## OPEN ACCESS

## RECEIVED

25 June 2014

## REVISED

27 August 2014

## ACCEPTED FOR PUBLICATION

29 August 2014

## PUBLISHED

10 February 2015

Content from this work  
may be used under the  
terms of the [Creative  
Commons Attribution 3.0  
licence](#).

Any further distribution of  
this work must maintain  
attribution to the author  
(s) and the title of the  
work, journal citation and  
DOI.

W Rowe<sup>1,2</sup>, I Eremin<sup>2,4</sup>, A T Rømer<sup>3</sup>, B M Andersen<sup>3</sup> and P J Hirschfeld<sup>1</sup><sup>1</sup> Department of Physics, University of Florida, Gainesville, USA<sup>2</sup> Institut für Theoretische Physik III, Ruhr-Universität Bochum, D-44801 Bochum, Germany<sup>3</sup> Niels Bohr Institute, University of Copenhagen, DK-2100 Copenhagen, Denmark<sup>4</sup> National University of Science and Technology 'MISIS', 119049 Moscow, RussiaE-mail: [wwang@ufl.edu](mailto:wwang@ufl.edu)

Keywords: superconductivity, cuprates, antiferromagnetism

## Abstract

We generalize the theory of Cooper-pairing by spin excitations in the metallic antiferromagnetic state to include situations with electron and/or hole pockets. We show that Cooper-pairing arises from transverse spin waves and from gapped longitudinal spin fluctuations of comparable strength. However, each of these interactions, projected on a particular symmetry of the superconducting gap, acts primarily within one type of pocket. We find a nodeless  $d_{x^2-y^2}$ -wave state is supported primarily by the longitudinal fluctuations on the electron pockets, and both transverse and longitudinal fluctuations support nodal  $d_{x^2-y^2}$ -wave symmetry on the hole pockets. Our results may be relevant to the asymmetry of the AF/SC coexistence state in the cuprate phase diagram.

## 1. Introduction

In contrast to the hole-doped cuprates, where quasi long-range static ( $\pi$ ,  $\pi$ ) antiferromagnetic (AF) order coexists with superconductivity (SC) only in the presence of disorder, electron-doped cuprates exhibit a homogeneous AF–SC coexistence phase [1]. This coexistence has been studied theoretically mostly with phenomenological interactions leading to the AF and SC order in cuprates [2–10] as well as in ferropnictides [11] and heavy fermions [12]. However, the microscopic foundation of the instability of the AF phase to SC due to pairing by itinerant electronic excitations is partially understood, thanks to early works by Schrieffer, Wen and Zhang [13], who generalized the theory of spin fluctuation pairing in weakly interacting Fermi liquids [14] and AF correlated metals [15] to the magnetically ordered phase. For example, while one might expect that low-energy AF spin waves could contribute substantially to pairing, it is known that the pairing vertex obeys a Ward identity, which prevents its divergence at the ordering wave vector, a property which is known as the Adler principle. It was further shown [17–20] that the net contribution of spin waves to the pairing vertex in the hole-doped systems was of the same order as that of longitudinal (gapped) spin and charge fluctuations, so both types of fluctuations must be included.

Although this classic problem has been the subject of theoretical scrutiny for twenty years, no general calculation of the evolution of the gap function across the phase diagram has been obtained. The original work of Schrieffer *et al* [13] and subsequent developments for hole-doped cuprates used a single band described by nearest-neighbor hopping  $t$  only and near half-filling. Here we analyze the full pairing interaction in the itinerant approach, including both longitudinal and transverse fluctuations, for a general Fermi surface and for both hole- and electron-doping. We develop a controlled analytical solutions for the leading pairing instability by projecting the effective spin–fluctuation interaction onto low-order circular harmonics of the small Fermi pockets, following the procedure proposed by Maiti *et al* [22]. For the hole-doped case, we find that the leading eigenvector of the linearized gap equation occurs with nodal  $d_{x^2-y^2}$ -wave symmetry in the spin singlet channel. In the case of electron doping, spin singlet nodeless  $d_{x^2-y^2}$ -wave pairing is the only channel that is strongly favored. Our findings have clear relevance for the topology of the overall phase diagram in the weak-coupling

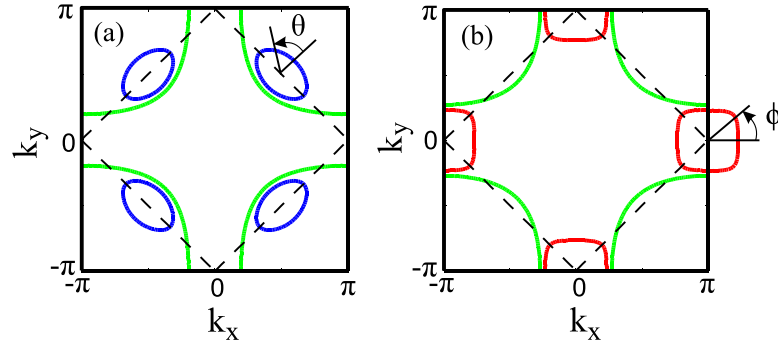


**Figure 1.** Structure of the Fermi surface topology in the commensurate AF state in layered cuprates for hole (a) or electron (b) doping. Here, we set  $t = 1$  and  $t' = 0.35t$ . The size of the hole pockets centered around  $(\pm\pi/2, \pm\pi/2)$  points of the BZ and the electron pockets around  $(\pm\pi, 0)$  and  $(0, \pm\pi)$  points of the BZ depends on the amount of doping. Here, we employ  $U = 2.775t$  and  $n = 0.95$  (a) and  $n = 1.10$  (b). The dashed line refers to the magnetic BZ boundary.

picture of the cuprates, since  $d_{x^2-y^2}$  Cooper-pairing can be easily suppressed by magnetic order only on the hole doped side, and the coexistence of AF and SC is found only upon electron doping.

## 2. Model

The commensurate AF state is treated in mean field for the single-band Hubbard model

$$\mathcal{H} = \sum_{\mathbf{k}\sigma} \varepsilon_{\mathbf{k}} c_{\mathbf{k}\sigma}^\dagger c_{\mathbf{k}\sigma} + \frac{1}{2} \sum_{\mathbf{k}, \mathbf{k}', \sigma} U c_{\mathbf{k}\sigma}^\dagger c_{\mathbf{k}+Q\sigma} c_{\mathbf{k}'+Q\sigma}^\dagger c_{\mathbf{k}'\sigma}, \quad (1)$$

on the square lattice with  $\varepsilon_{\mathbf{k}} = -2t(\cos k_x + \cos k_y) + 4t' \cos k_x \cos k_y - \mu$ , with  $t$  and  $t'$  the nearest and next nearest hoppings. After decoupling the second term via a mean-field (MF) approximation and diagonalizing the resulting Hamiltonian via unitary transformation, we obtain two electronic bands (labeled  $\alpha$  and  $\beta$ ) in the reduced (magnetic) Brillouin zone (rBZ) with dispersions  $E_{\mathbf{k}}^{\alpha\beta} = \varepsilon_{\mathbf{k}}^\pm \pm \sqrt{(\varepsilon_{\mathbf{k}}^-)^2 + W^2}$  where  $W = U/2 \sum_{\mathbf{k}', \sigma} \langle c_{\mathbf{k}'+Q\sigma}^\dagger c_{\mathbf{k}'\sigma} \rangle \text{sgn } \sigma$  is the AF order parameter, determined self-consistently for a given  $U$ , and  $\varepsilon_{\mathbf{k}}^\pm = (\varepsilon_{\mathbf{k}} \pm \varepsilon_{\mathbf{k}+Q})/2$ . For completeness, one also has to include the self-consistent determination of the chemical potential.

Typical Fermi surfaces in the AF metal for the case of electron and hole dopings are then shown in figure 1. Note that for small electron doping only electron pockets at  $(\pm\pi, 0)$  and  $(0, \pm\pi)$  are present, while for hole doping only hole pockets around  $(\pm\pi/2, \pm\pi/2)$  can occur. For intermediate values of electron doping and finite temperatures both types of pockets can appear.

The effective Hamiltonian in the paramagnetic state  $\mathcal{H} = \mathcal{H}_c + \mathcal{H}_z + \mathcal{H}_\pm$  is obtained by summing all random phase approximation (RPA) type processes in the charge, longitudinal spin and transverse spin-fluctuation channels [13].

$$\begin{aligned} \mathcal{H}_c &= \frac{1}{4} \sum_{\mathbf{k}, \mathbf{k}', \mathbf{q}} [2U - V_{\mathbf{k}-\mathbf{k}'}^c] c_{\mathbf{k}s_1}^\dagger c_{-\mathbf{k}'+\mathbf{q}s_2}^\dagger c_{-\mathbf{k}+\mathbf{q}s_2} c_{\mathbf{k}s_1}, \\ \mathcal{H}_z &= -\frac{1}{4} \sum_{\mathbf{k}, \mathbf{k}', \mathbf{q}} V_{\mathbf{k}-\mathbf{k}'}^z \sigma_{s_1, s_2}^3 \sigma_{s_3, s_4}^3 c_{\mathbf{k}'s_1}^\dagger c_{-\mathbf{k}'+\mathbf{q}s_3}^\dagger c_{-\mathbf{k}+\mathbf{q}s_4} c_{\mathbf{k}s_2}, \\ \mathcal{H}_\pm &= -\frac{1}{4} \sum_{\mathbf{k}, \mathbf{k}', \mathbf{q}} V_{\mathbf{k}-\mathbf{k}'}^\pm (\sigma_{s_1, s_2}^+ \sigma_{s_3, s_4}^- + \sigma_{s_1, s_2}^- \sigma_{s_3, s_4}^+) \\ &\quad \times c_{\mathbf{k}'s_1}^\dagger c_{-\mathbf{k}'+\mathbf{q}s_3}^\dagger c_{-\mathbf{k}+\mathbf{q}s_4} c_{\mathbf{k}s_2}, \end{aligned} \quad (2)$$

where the interactions are expressed in terms of the various components of the bare charge and spin susceptibilities,  $V^c = \frac{U^2 \chi_0^0}{1 + U \chi_0^0}$ ,  $V^z = \frac{U^2 \chi_0^z}{1 - U \chi_0^z}$  and  $V^\pm = \frac{U^2 \chi_0^\pm}{1 - U \chi_0^\pm}$ . The bare charge susceptibility  $\chi^0$  and the bare spin longitudinal susceptibility have the same values in the pure AF state. The susceptibilities  $\chi^0$ ,  $\chi^z$  and  $\chi^\pm$  are functions of  $\mathbf{k}-\mathbf{k}'$ .

We now perform a change of basis to the eigenstates of the AF state, the so-called  $\alpha$  and  $\beta$  bands [8]. The corresponding effective *intra*band ( $\alpha\alpha$  or  $\beta\beta$ ) interactions in the singlet and triplet channels  $\Gamma_0(\mathbf{k}, \mathbf{k}')$  and  $\Gamma_1^{z/x, y}(\mathbf{k}, \mathbf{k}')$  are expressed as

$$\Gamma_0 = \Gamma_\rho - \Gamma_s^z - 2\Gamma_s^\perp, \quad (3)$$

$$\Gamma_1^z = \Gamma_\rho - \Gamma_s^z + 2\Gamma_s^\perp, \quad (4)$$

$$\Gamma_1^{x,y} = \Gamma_\rho + \Gamma_s^z - 2U(l^2 + m^2), \quad (5)$$

in terms of the charge, spin longitudinal and spin transverse vertices

$$\begin{aligned} \Gamma_\rho(\mathbf{k}, \mathbf{k}') &= [2U - V_{\mathbf{k}-\mathbf{k}'}^c]l^2 - [V_{\mathbf{k}-\mathbf{k}'+\mathbf{Q}}^z]m^2, \\ \Gamma_s^z(\mathbf{k}, \mathbf{k}') &= [2U - V_{\mathbf{k}-\mathbf{k}'+\mathbf{Q}}^c]m^2 - [V_{\mathbf{k}-\mathbf{k}'}^z]l^2, \\ \Gamma_s^\perp(\mathbf{k}, \mathbf{k}') &= -[V_{\mathbf{k}-\mathbf{k}'}^\pm]n^2 + [V_{\mathbf{k}-\mathbf{k}'+\mathbf{Q}}^\pm]p^2. \end{aligned} \quad (6)$$

Here, the coherence factors induced by the unitary transformations are given by

$$\begin{aligned} m^2(\mathbf{k}, \mathbf{k}') &= \frac{1}{2} \left[ 1 - \frac{\varepsilon_{\mathbf{k}}^- \varepsilon_{\mathbf{k}'}^- - W^2}{\sqrt{(\varepsilon_{\mathbf{k}}^-)^2 + W^2} \sqrt{(\varepsilon_{\mathbf{k}'}^-)^2 + W^2}} \right], \\ l^2(\mathbf{k}, \mathbf{k}') &= \frac{1}{2} \left[ 1 + \frac{\varepsilon_{\mathbf{k}}^- \varepsilon_{\mathbf{k}'}^- + W^2}{\sqrt{(\varepsilon_{\mathbf{k}}^-)^2 + W^2} \sqrt{(\varepsilon_{\mathbf{k}'}^-)^2 + W^2}} \right], \\ p^2(\mathbf{k}, \mathbf{k}') &= \frac{1}{2} \left[ 1 - \frac{\varepsilon_{\mathbf{k}}^- \varepsilon_{\mathbf{k}'}^- + W^2}{\sqrt{(\varepsilon_{\mathbf{k}}^-)^2 + W^2} \sqrt{(\varepsilon_{\mathbf{k}'}^-)^2 + W^2}} \right], \\ n^2(\mathbf{k}, \mathbf{k}') &= \frac{1}{2} \left[ 1 + \frac{\varepsilon_{\mathbf{k}}^- \varepsilon_{\mathbf{k}'}^- - W^2}{\sqrt{(\varepsilon_{\mathbf{k}}^-)^2 + W^2} \sqrt{(\varepsilon_{\mathbf{k}'}^-)^2 + W^2}} \right]. \end{aligned} \quad (7)$$

There are also *interband* ( $\alpha^\dagger \alpha^\dagger \beta \beta + \text{h.c.}$ ) pair scattering interactions  $\Gamma_0'$  and  $\Gamma_1^{z,x/y}$ , which are identical in form to the *intra-band* vertices with  $m^2 \leftrightarrow n^2$  and  $p^2 \leftrightarrow \ell^2$ . In addition, the Cooper-pairing vertex is taken to be symmetrized and antisymmetrized with respect to  $\mathbf{k}'$  in the spin singlet ( $0.5[\Gamma_0(\mathbf{k}, \mathbf{k}') + \Gamma_0(-\mathbf{k}, \mathbf{k}')]$ ) and spin triplet ( $0.5[\Gamma_1^{z,x/y}(\mathbf{k}, \mathbf{k}') - \Gamma_1^{z,x/y}(-\mathbf{k}, \mathbf{k}')]$ ) channels, respectively.

Another important consequence of the AF state is that the spin rotational symmetry present in the paramagnetic state is broken, and all components of the susceptibility are different [13, 17, 18, 26]. While the transverse component is gapless and shows a Goldstone mode with spin wave excitations around the AF wave vector, the longitudinal spin excitations are gapped up to twice the AF gap magnitude. The behavior of the spin excitations in the AF state is well understood including the effect of  $t'$  as well as their doping dependence, see e.g. [26].

Note that despite the fact that the spin rotational symmetry is broken in the AF state, the Cooper-pairing vertices in the spin triplet and the spin singlet channels remain well separated. This is a consequence of the fact that the inversion symmetry is still preserved. However, an additional contribution to Cooper-pairing due to Umklapp terms,  $\langle c_{\mathbf{k},\uparrow} c_{-\mathbf{k}-\mathbf{Q},\downarrow} \rangle$ , present in the AF state only, has opposite symmetry, when written in terms of the original  $c$  operators. Namely, one finds that terms  $\langle c_{\mathbf{k},\uparrow} c_{-\mathbf{k}-\mathbf{Q},\downarrow} \rangle$  contributing to the spin singlet vertex in the AF background would have a spin triplet symmetry in the paramagnetic state and vice versa.

An important property of the spin singlet Cooper-pairing in the AF background is that the fluctuation exchange pairing potentials have the symmetry  $\Gamma_0(\mathbf{k}, \mathbf{k}' + \mathbf{Q}) = \Gamma_0(\mathbf{k} + \mathbf{Q}, \mathbf{k}') = -\Gamma_0(\mathbf{k}, \mathbf{k}')$ . Note that this symmetry is also fulfilled for the opposite spin triplet potential  $\Gamma_1^z$ , as well as for transverse and longitudinal parts of the fluctuations separately. This requires that any solution for the superconducting gap function changes sign for  $\mathbf{k} \rightarrow \mathbf{k} + \mathbf{Q}$  [13]. Therefore, it excludes isotropic s-wave as well as  $d_{xy}$  symmetries of the superconducting gap. In the spin singlet channel this yields extended s-wave symmetry with the gap changing sign across the rBZ boundary, or  $d_{x^2-y^2}$ -wave symmetry which in this case is compatible with the condition  $\Gamma_0(\mathbf{k}, \mathbf{k}' + \mathbf{Q}) = -\Gamma_0(\mathbf{k}, \mathbf{k}')$  without any gap nodes at the rBZ boundary. In the opposite spin triplet channel, this condition allows p-wave solutions with  $\sin k_x$  or/and  $\sin k_y$  form [13]. The equal spin triplet vertices obey an analogous sublattice symmetry without the sign change,  $\Gamma_1^{x,y}(\mathbf{k}, \mathbf{k}' + \mathbf{Q}) = \Gamma_1^{x,y}(\mathbf{k} + \mathbf{Q}, \mathbf{k}') = \Gamma_1^{x,y}(\mathbf{k}, \mathbf{k}')$ . It is important to note that there are clearly two different contributions to Cooper-pairing for low frequencies. The first arises from the transverse fluctuations which is dominated by the spin waves at the AF momentum, and the second is a

combination of the longitudinal spin and charge fluctuations. To analyze the dominant instabilities further, we study both small electron and hole doping.

### 3. Small pocket expansion

To proceed analytically, we assume small sizes of the electron and hole pockets and expand the pairing interactions including the AF coherence factors as well as the possible superconducting gaps, extended s-wave with form similar to  $\cos k_x + \cos k_y$ ,  $d_{x^2-y^2}$ -wave with  $\cos k_x - \cos k_y$  in the spin singlet channel, and odd parity p-wave with  $\sin k_x$  [ $\sin k_y$ ] dependence in the opposite spin singlet channel, respectively, around the corresponding momenta. We assume the pockets to be circular and expand the interaction in terms of angular harmonics up to order  $k_F^2$ , writing them in terms of the  $\cos n\theta$  and  $\cos n\phi$  where the angles  $\theta$  and  $\phi$  are defined in figure 1. The deviation of pockets from being circular will enhance the corresponding higher order angular harmonics terms in the interaction but will not change the overall gap structure itself.

Taking into account the symmetry of the pairing interaction on the background of the AF state in the rBZ, it is sufficient to consider only three pockets, one electron pocket which we choose to lie at  $(\pi, 0)$  ( $e$ ) and two hole pockets which we take at  $(\pi/2, \pi/2)$  ( $h_1$ ) and  $(-\pi/2, \pi/2)$  ( $h_2$ ). All others are automatically included by performing the angular integration over the angles and bearing in mind the properties of the pairing potential and gap under  $\mathbf{k} \rightarrow \mathbf{k} + \mathbf{Q}$ . For extended s-wave symmetry we find

$$\begin{aligned}\Delta_{h_1}^s(\theta) &= \Delta_h^s \cos \theta, \quad \Delta_{h_2}^s(\theta) = \Delta_h^s \sin \theta, \\ \Delta_e^s(\phi) &= \Delta_e^s \cos 2\phi,\end{aligned}\quad (8)$$

where the angles are defined in figure 1. Equation (8) shows that the gap generally has nodes on both electron and hole pockets. In addition the gap on the electron pocket has  $\cos 2\phi$  dependence as a result of the expansion of the  $\cos k_x + \cos k_y$  wave function around  $(\pi, 0)$ .

For the  $d_{x^2-y^2}$  channel, the expansion gives the following form of the gaps on the electron and hole pockets

$$\begin{aligned}\Delta_{h_1}^d(\theta) &= \Delta_h^d \sin \theta, \quad \Delta_{h_2}^d(\theta) = \Delta_h^d \cos \theta, \\ \Delta_e^d(\phi) &= \Delta_e^d (1 + \alpha_e^d \cos 4\phi).\end{aligned}\quad (9)$$

Here, the gap on the hole pockets is nodal, while on the electron ones the first term is a constant.

Finally, the symmetry properties of the spin triplet Cooper-pairing allow for the p-wave nodeless solution for the hole pockets. In this case the gap (either  $\sin k_x$  or  $\sin k_y$ ) may be expanded around the hole pockets

$$\begin{aligned}\Delta_{h_1}^p(\theta) &= \Delta_h^p \\ \Delta_{h_2}^p(\theta) &= \pm \Delta_h^p \\ \Delta_e^p(\phi) &= \Delta_e^p \sin \phi [\cos \phi]\end{aligned}\quad (10)$$

The  $\pm$  sign refers to two distinct p-wave states.

#### 3.1. Longitudinal spin and charge interactions

In a similar fashion, we now expand the effective pairing interaction between opposite spin electrons in the transverse and longitudinal/charge channels, equations (3)–(4). For the longitudinal/charge channel contribution to the spin singlet and opposite spin triplet Cooper-pair scattering  $V^\ell \equiv \Gamma_\rho - \Gamma_s^z$ , one finds for the interaction within hole and electron pockets,

$$\begin{aligned}V_{h_1 h_1}^1(\theta, \theta') &\approx c_h + a_h \cos \theta \cos \theta' + b_h \sin \theta \sin \theta' \\ &\quad + c_h (\cos 2\theta + \cos 2\theta'), \\ V_{h_2 h_2}^1(\theta, \theta') &\approx c_h + a_h \sin \theta \sin \theta' + b_h \cos \theta \cos \theta' \\ &\quad + c_h (\cos 2\theta + \cos 2\theta'), \\ V_{ee}^1(\phi, \phi') &\approx c_e + d_e (\cos \phi \cos \phi' + \sin \phi \sin \phi'),\end{aligned}\quad (11)$$

where  $c_h \equiv \tilde{V} + [\tilde{V} - \frac{2r^2\tilde{V}}{w^2}]k_F^2$ ,  $a_h \equiv [-\tilde{V} + \frac{4t^2\tilde{V}}{w^2}]k_F^2$ ,  $b_h \equiv \tilde{V}k_F^2$ ,  $c_e \equiv \tilde{V} + \tilde{V}k_F^2$ ,  $d_e \equiv \tilde{V}k_F^2$ , with  $Y(x) = 4U \frac{\chi_0^z(x)V_z(x)}{1 + U\chi_0^z(x)} (1 + \frac{V_z(x)^2 U^{-2}}{(1 + U\chi_0^z(x))^2})$ , where  $\chi_0^z$  is the second derivative of the bare longitudinal spin

susceptibility,  $\tilde{V} \equiv [V_z(0) - V_c(0) + (V_c(Q) - V_z(Q))]$ , and  $\tilde{V} \equiv Y(0) - Y(Q)$ . Note that  $\tilde{V}$  is negative (attractive), since  $V_z(Q)$  is the largest term and the same is true for  $\tilde{V}$ . In addition, note that the coefficients  $c_h$  and  $d_e$  appear to have odd symmetry under the change of  $\mathbf{k}$  to  $-\mathbf{k}$  (or  $\mathbf{k}'$  to  $-\mathbf{k}'$ ), which can be seen by doing the

explicit analysis. Thus, they contribute only to the triplet Cooper-pairing. At the same time  $a_h, b_h,$  and  $c_e$  possess even symmetry and contribute to the spin singlet symmetry. In both cases, the dominant contribution is given by the constant term  $c_{h,e}$ , independent of the pocket type. In addition, this constant term is almost independent of the pocket size and, therefore, yields the dominant contribution from longitudinal spin fluctuations. Most importantly, it does not give rise to a conventional s-wave state due to the sublattice symmetry of  $V(\mathbf{k}, \mathbf{k}')$  mentioned above. Looking at the expansion of the superconducting gaps, equations (7)–(9), one sees that the constant term from the longitudinal spin fluctuations contributes mostly to the  $d_{x^2-y^2}$ -wave pairing on the electron pockets, while on the hole pockets it may give rise to one of the two nodeless odd-parity p-wave states [13]. However, because the triplet pairing contribution from the transverse potential is repulsive on the hole pocket as we shall see below in equation (12), the possible solution might be an f-wave (not shown) rather than p-wave. For the hole pockets, there is a leading projection onto the  $d_{x^2-y^2}$ -wave state that scales with the sizes of the hole pockets  $(k_F^h)^2$ .

### 3.2. Transverse spin interaction

For the transverse part of the pairing vertex the expansion is more subtle, since the coefficients of the unitary transformation  $(p^2, n^2)$  are such that for any  $\mathbf{k}' \approx \mathbf{k}$  they tend to zero, as required by the Adler principle. However, the total pairing vertex in the transverse channel is non-zero as the smallness of  $p^2, n^2$  is compensated by the diverging transverse part of the spin susceptibility  $V^{\text{tr}} \equiv -2\Gamma_s^\perp \sim \chi_{\text{RPA}}^\pm$ , and overall there is a contribution of the spin waves to the pairing vertex which is also independent of the sizes of the electron and hole pockets, similar to the longitudinal channel [17–21]. It is easy to check from equations (3)–(4) that the transverse spin fluctuation contribution to the pairing vertex has the same magnitude but opposite sign in the spin singlet,  $\Gamma_0$ , and the spin triplet,  $\Gamma_1^z$  Cooper-pairing, respectively.

To obtain the leading angular harmonics in the spin singlet and spin triplet pairing channels due to transverse spin fluctuations, we expand both the coefficients of the unitary AF transformations entering  $\Gamma_s^\perp$ , as well as the diverging part of the spin susceptibility at  $\mathbf{Q}$  up to  $q^2$  and combine them together. The expansion for  $V^{\text{tr}} \equiv 2\Gamma_s^\perp$  then has the following form:

$$\begin{aligned} V_{h1h1}^{\text{tr}}(\theta, \theta') &\approx A_h(\pm 1 - \cos \theta \cos \theta' + \sin \theta \sin \theta') \\ &\quad + B_h(\pm 2 + 4 \cos \theta \cos \theta' \pm \cos 2\theta \pm \cos 2\theta'), \\ V_{h2h2}^{\text{tr}}(\theta, \theta') &\approx A_h(\pm 1 + \cos \theta \cos \theta' - \sin \theta \sin \theta') \\ &\quad + B_h(\pm 2 + 4 \sin \theta \sin \theta' \mp \cos 2\theta \mp \cos 2\theta'), \\ V_{ee}^{\text{tr}}(\phi, \phi') &\approx A_e(1 \pm \cos \phi \cos \phi' \pm \sin \phi \sin \phi') \\ &\quad \mp \frac{1}{2}(\cos 3\phi \cos \phi' - \sin 3\phi \sin \phi' + \cos \phi \cos 3\phi' - \sin \phi \sin 3\phi') \\ &\quad - \cos 2\phi \cos 2\phi' + \sin 2\phi \sin 2\phi'), \end{aligned} \quad (12)$$

where in terms of

$$\begin{aligned} y &= \frac{16}{N} \sum_{\mathbf{k}} \frac{\sin^2 k_x \left( 1 - 6 \frac{(\varepsilon_{\mathbf{k}})^2}{(E_{\mathbf{k}}^\alpha - E_{\mathbf{k}}^\beta)^2} \right) - \frac{1}{2} \cos^2 k_x - \frac{1}{2} \cos k_x \cos k_y}{(E_{\mathbf{k}}^\alpha - E_{\mathbf{k}}^\beta)^3} \\ &\quad - \frac{32(t')^2}{t^2 N} \sum_{\mathbf{k}} \frac{\sin^2 k_x \cos^2 k_y}{(E_{\mathbf{k}}^\alpha - E_{\mathbf{k}}^\beta)^3}, \end{aligned}$$

we have  $A_h \equiv \frac{2}{yW^2}$ ,  $B_h \equiv V_\pm(0)(\frac{tk_F^h}{W})^2$ , and  $A_e \equiv \frac{k_F^e}{2yW^2}$ . Here,  $y$  is related to the spin wave stiffness and is positive once commensurate AF order is stable. In addition,  $+-$  and  $-+$  refer to the odd-parity terms which change sign under the  $\mathbf{k}$  to  $-\mathbf{k}$  or  $\mathbf{k}'$  to  $-\mathbf{k}'$  transformations. They contribute to the spin triplet Cooper-pairing only, while other terms contribute to the spin singlet Cooper-pairing. Note that for spin singlet Cooper-pairing the overall sign of the transverse pairing interaction is reversed, as seen from equation (3).

## 4. Discussion

In this section, we now use what we have learned above about the spin fluctuation pairing interaction in the limit of small electron or hole pockets to determine the leading pairing channel in various cases. It is worth noting that, while a great deal of work went into studying the properties of this interaction in the AF state, ultimately all

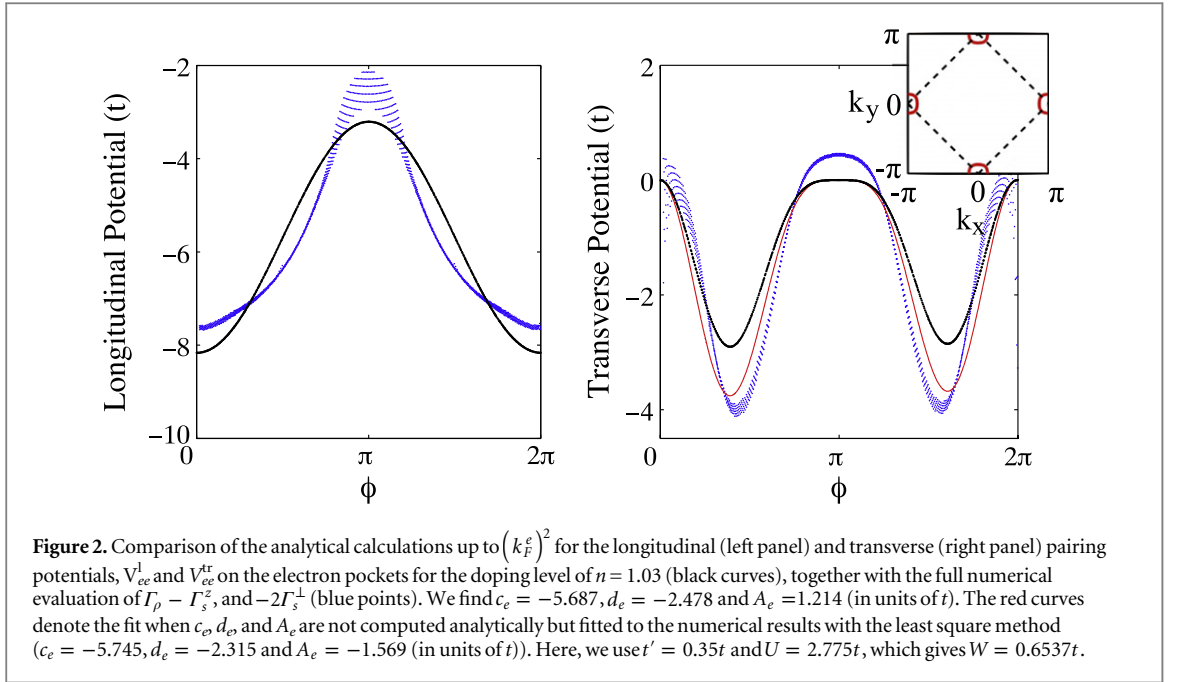


**Table 1.** Contribution of the spin fluctuation mediated Cooper-pairing potential, expanded up to  $O(k_F^e)$  terms, in the  $p$ -wave spin triplet channel.

	Electron pocket		Hole Pocket	
	long./ch.	transverse	long./ch.	transverse
Pair-building contribution	$d_e \sim O((k_F^e)^2)$	—	$c_h \sim O(1)$	—
Pair-breaking contribution	—	$A_e \sim O((k_F^e)^2)$	—	$A_h \sim O(1)$

previous workers in this field did not address this problem explicitly, but simply listed the possible states consistent with sublattice symmetry.

We begin by noting that an important difference between the transverse fluctuations and the charge and longitudinal spin fluctuations is that the former contribute mostly to the Cooper-pairing for the hole pockets. In particular, the leading spin-wave contribution to the pairing vertex does not depend on the sizes of the hole pockets, while around the electron pockets it is reduced in strength by the smallness of these pockets, i.e. it vanishes for  $k_F^e \rightarrow 0$ . This indicates that the longitudinal and transverse spin fluctuations act differently in the different parts of the rBZ. While the charge and longitudinal spin fluctuations contribute equally to the Cooper-pairing around  $(\pi, 0)$  and  $(\pi/2, \pi/2)$ , the low-energy transverse fluctuations are most effective around  $(\pm\pi/2, \pm\pi/2)$ . Furthermore, as both types of fluctuation do not contribute to the interband Cooper-pair scattering until higher order in  $k_F$ , the same remains true also in the situation when both electron and hole type pockets are present at the Fermi surface. To see how the analytical calculations agree with the full numerical ones, we show in figure 2 the good agreement of the analytical calculations for the longitudinal and transverse pairing potentials,  $V_{ee}^l$  and  $V_{ee}^{tr}$  on the electron pockets for the doping level of  $n = 1.03$ , together with the numerical evaluation of  $\Gamma_\rho - \Gamma_s^z$ , and  $-2\Gamma_s^\perp$ . We also compare with a low-order harmonic fit to the numerical results with the coefficients  $c_e$ ,  $d_e$ , and  $A_e$  treated as independent.

#### 4.1. Pairing instability for electron- and hole-doping

Overall the results shown in (11)–(12) for the leading expansion coefficients up to quadratic order in the Fermi momentum that contribute to the spin singlet and spin triplet Cooper-pairing channels are summarized in tables 1 and 2. Regarding the dominant pairing instability, the situation is clear for the electron pocket at  $(\pi, 0)$  by simply projecting the longitudinal part of the Cooper-pairing vertex (11), which dominates in this limit as shown above, onto the gaps (8)–(10) in the linearized superconducting gap equation



**Table 2.** Contribution of the spin fluctuation mediated Cooper-pairing potential, expanded up to  $O(k_F^2)$  terms, in the spin-singlet  $d_{x^2-y^2}$ -wave channel. Note that all contributions in the extended  $s$ -wave symmetry channel are pair-breaking.

	Electron pocket		Hole Pocket	
	long./ch.	transverse	long./ch.	transverse
Pair-building, $d_{x^2-y^2}$ – wave symmetry	$c_e \sim O(1)$	$A_e \sim O((k_F^e)^2)$	$b_h \sim O((k_F^h)^2)$	$A_h \sim O(1)$

$$\lambda_e \Delta_e(\phi) = - \int_{\phi'} \frac{N_e}{2\pi} \Gamma_{0,1}(\phi, \phi') \Delta(\phi'), \quad (13)$$

where  $N_e$  is the density of states on the electron pockets and the angular integral runs over all relevant pockets. The constant part of the longitudinal spin fluctuations,  $c_e$  in equation (11), is attractive in the spin singlet channel and gives rise to the  $d_{x^2-y^2}$ -wave symmetry of the superconducting order parameter, which can also be approximated by a constant on the electron pockets with appropriate sign changes from pocket to pocket enforced by sublattice symmetry. The  $d$ -wave state is nodeless due to the placement of the electron pockets at the  $(\pi, 0)$  points. The first non-vanishing higher order harmonic is in this case  $4\phi$ , which can be also promoted by the longitudinal and transverse spin fluctuations, weakened by the  $(k_F^e)^2$  factor. In principle, longitudinal spin fluctuations are also attractive in the opposite spin triplet channel, however the  $\sin k_x$  or  $\sin k_y$  function does not have an angle-independent constant term in the expansion around the  $(\pi, 0)$  and  $(0, \pi)$  points.

The situation is more complicated for the hole pockets, where contributions from both longitudinal and transverse channels remain in the limit of small  $k_F^h$ . The largest part of the pairing vertex, which originates from the transverse spin fluctuations, is attractive also only in the  $d_{x^2-y^2}$ -wave channel.

#### 4.2. Comparison with the strong-coupling limit

It is interesting to compare our results with the strong-coupling limit, studied extensively in the past [19, 20]. The important advantage of the weak-coupling scenario is that one can verify the evolution of the spin fluctuation Cooper-pairing from the paramagnetic to the AF states continuously as a function of the AF order parameter magnitude, while in the strong coupling approach the transition from the AF to the paramagnetic limit cannot be taken continuously (at least we are not aware of such a study in the literature).

Let us note that the strong and weak coupling approaches agree qualitatively for hole-doping with hole pockets around  $(\pm\pi/2, \pm\pi/2)$ , and for electron-doping with pockets around  $(\pm\pi, 0)$  and  $(0, \pm\pi)$ , both strong and weak-coupling approaches give similar results with  $d_{x^2-y^2}$ -wave symmetry being most dominant one. Therefore let us illustrate the situation for the hole pockets. In this case the main contribution to the Cooper-pairing comes indeed from the transverse spin fluctuations and it is easy to verify the following relation for the coherence factors  $p^2(\mathbf{k} + \mathbf{Q}, \mathbf{k}') = p^2(\mathbf{k}, \mathbf{k}' + \mathbf{Q}) = n^2(\mathbf{k}, \mathbf{k}')$ . This results in the antiperiodic condition for the total transverse potential  $\Gamma_s^\perp(\mathbf{k}, \mathbf{k}' + \mathbf{Q}) = -\Gamma_s^\perp(\mathbf{k}, \mathbf{k}')$  where one needs both terms of the pairing potential to satisfy the total antiperiodicity of the potential. This antiperiodicity of the potential requires also the antiperiodicity of the superconducting gap,  $\Delta_s(\mathbf{k} + \mathbf{Q}) = -\Delta_s(\mathbf{k})$  in order to fulfill the gap equation. This excludes the isotropic  $s$ -wave solution for the superconducting gap in the entire magnetic BZ.

An important difference between the weak-coupling and the strong-coupling approaches is related to the definition of the problem. In the latter case one considers the problem of the Cooper-pairing for the fermions due to Goldstone excitations (spin waves) without taking into account the unitary transformations of the fermions from the paramagnetic to the AF state. In this case the fermions are considered to be the bare ones, that is, they are not dressed by the AF coherence factors. In the weak-coupling approach, one finds two contributions to the transverse pairing vertex  $\Gamma_s^\perp$  in equation (6), and the second one occurs due to Umklapp Cooper-pairs (in other words, in terms of the original  $c$  operators in the paramagnetic state, this corresponds to Cooper-pairing with large  $\mathbf{Q}$  momentum transfer, i.e.  $c_{k\uparrow} c_{-k-\mathbf{Q}\downarrow}$ ). This pairing is absent in the paramagnetic state and exists only if the AF gap is non-zero. In addition, if both  $\mathbf{k}$  and  $\mathbf{k}'$  are small, i.e. we consider only one hole pocket centered at  $(\pi/2, \pi/2)$ , such that the spin waves contribute only to the second term, since  $[V_{+-}(\mathbf{k} - \mathbf{k}' + \mathbf{Q})] p^2(\mathbf{k}, \mathbf{k}')$  contains the susceptibility peaked at the wavevector  $\mathbf{Q}$  where the true Goldstone mode arises. As we said, due to antiperiodicity of the total pairing vertex this term cannot stabilize the global isotropic  $s$ -wave solution in the entire magnetic BZ. For the Fermi surface topology with small hole pockets, the pairing potential expanded near the pocket gives rise to the conventional nodal spin singlet  $d_{x^2-y^2}$ -wave solution and odd parity  $f$ -wave solution. The  $d_{x^2-y^2}$  state is forced to have nodes on the hole pockets. We note that in the strong-coupling case, both  $p$ -wave and  $d_{x^2-y^2}$ -wave solutions were found; however, the details of the competition between these states were

not analyzed [19, 20]. In this regard, we believe that the analysis of the strong coupling is still not complete, as the limiting case of the AF gap going to zero is not well understood there.

At the same time, in the weak-coupling limit an inclusion of the self-energy effects due to the coupling of transverse spin fluctuations to conduction electrons also introduces significant corrections to the properties of the magnetic state like a renormalization of the magnitude of the magnetic order parameter, and the spin wave velocity [27, 28]. Furthermore, for small  $U$ , the effective interaction between quasiparticles is of the order of the bandwidth in the transverse channel and so both vertex and self-energy corrections are relatively small [28]. In this limit, one might expect that the MF treatment of the magnetic state leads to at least qualitatively correct results. On the contrary, for large  $U$  the interaction is much larger than the bandwidth of both the holes and the spin waves. This corresponds more to the strong-coupling situation in which one has strong vertex and self-energy renormalization. It is known that at finite hole doping this effectively yields an instability of the AF state with commensurate order with respect to the spiral magnetic state [28]. These effects we also found previously in the weak-coupling case, where the spin wave spectrum becomes unstable for finite hole-doping [26]. Here, we assume that the coupling of the transverse spin fluctuations to the conduction electrons do not change the results significantly, which should be true in the weak to intermediate coupling regimes.

We observe also that the gap equation in the AF state reduces correctly in the weak-coupling approach to the gap equation in the paramagnetic state. For the limiting case of an AF gap going to zero, one finds that the second term in the pairing vertex vanishes and the only remaining contribution comes from the first term, which refers to the non-Goldstone large  $Q$  repulsive spin fluctuations. These fluctuations in the paramagnetic state give rise to the  $d_{x^2-y^2}$ -wave solution for the superconducting gap on the hole-doped and electron-doped sides of the phase diagram with large Fermi surfaces. An important difference, however, is that in contrast to the hole-doped side the  $d_{x^2-y^2}$ -wave solution on the electron-doped counterpart cannot be fitted by the lowest  $\cos 2\phi$  harmonic of the superconducting gap due to the position of the hot spots on the Fermi surface close to the diagonal of the rBZ. Analytically, this continuation is straightforward to see, however; numerically there are some complications at finite doping mostly on the hole-doped side related to the instability of the commensurate magnetic order against incommensurate spiral AF state once hole pockets appear on the Fermi surface. As a result, the computations become more involved and the complete numerical phase diagram cannot be obtained at this stage. Nevertheless, we see that the superconducting transition temperatures will be smaller in the AF state than in the paramagnetic state. In the presence of both the transverse and longitudinal fluctuations the main effect on the superconducting gap and  $T_c$  will be determined by the smallness of the electron and the hole pocket size. These will be determined by the amount of doping,  $x$ , and  $T_c$  will scale with this quantity.

## 5. Summary

In summary, we have discussed the important ways in which the pairing instability in the AF state differs between the electron- and hole-doped cases. When long-range AF order occurs, the fluctuations which generically lead to  $d_{x^2-y^2}$ -wave pairing in the paramagnetic state for systems with a cuprate-like Fermi surface are frozen out. We have shown that the residual fluctuations turn out to be quite strong in the case of electron pockets, and remain constant in the  $d_{x^2-y^2}$ -wave channel even in the limit of small pockets (large magnetization), yielding a nodeless d-wave ground state. In the hole-doped case, the pairing due to these residual fluctuations is constant in the limit of small hole pockets in both the singlet and triplet channel. It is strongest for (nodal)  $d_{x^2-y^2}$ -wave symmetry, and much weaker in the spin triplet channel, due to a near cancellation of contributions from longitudinal and transverse channels.

We emphasize that our rigorous conclusions do *not* apply generically to the entire range of dopings and temperatures, but only to the limit of small Fermi surface pockets (large magnetization). A full calculation of the microscopic phase diagram including the free energy analysis requires a treatment of SC and magnetism in the ordered state on equal footing, including the renormalization of the AF instability in the case  $T_N < T_c$ , which is beyond the scope of this work.

It is also important to mention that our results in the weak-coupling limit for the symmetry of the Cooper-pairing are consistent with those found in the strong-coupling limit [29]. In particular, in the strong-coupling limit the dominant symmetry remains also  $d_{x^2-y^2}$ -wave. This result does not change in the weak-coupling where the contribution of the longitudinal spin fluctuations, ignored in the strong-coupling approach, is also included.

## Acknowledgments

We acknowledge helpful discussions with Ph Brydon, W Cho, AV Chubukov, S Kivelson, J Knolle, and O Sushkov. WR and PJH were supported by NSF-DMR-1005625. WR is grateful for the hospitality of the Ruhr-

University Bochum and PJH to Goethe-Universität Frankfurt, where the final stage of this work was performed. This work was supported by the Focus Program 1458 ‘Eisen-Pniktide’ of the DFG, and by the German Academic Exchange Service (DAAD PPP USA no. 57051534). IE acknowledges the financial support of the Ministry of Education and Science of the Russian Federation in the framework of Increase Competitiveness Program of NUST MISiS (N 2–2014–015). BMA acknowledges support from the Lundbeckfond fellowship (grant A9318).

## References

- [1] Armitage N P, Fournier P and Greene R L 2010 *Rev. Mod. Phys.* **82** 2421
- [2] Inui M, Doniach S, Hirschfeld P J and Ruckenstein A E 1988 *Phys. Rev. B* **37** 2320
- [3] Murakami M and Fukuyama H 1998 *J. Phys. Soc. Japan* **67** 2784
- [4] Kulic M L, Lichtenstein A I, Goreatchkovski E and Mehring M 1995 *Physica C* **244** 185
- [5] Yamase H and Kohno H 2004 *Phys. Rev. B* **69** 104526
- [6] Kyung B 2000 *Phys. Rev. B* **62** 9083
- [7] Reiss J, Rohe D and Metzner W 2007 *Phys. Rev. B* **75** 075110
- [8] Ismer J-P, Eremin I, Rossi E, Morr D K and Blumberg G 2010 *Phys. Rev. Lett.* **105** 037003
- [9] Das T, Markiewicz R S, Bansil A and Balatsky A V 2012 *Phys. Rev. B* **85** 224535
- [10] Cho W, Thomale R, Raghu S and Kivelson S A 2013 *Phys. Rev. B* **88** 064505
- [11] Vorontsov A B, Vavilov M G and Chubukov A V 2010 *Phys. Rev. B* **81** 174538  
Fernandes R M and Schmalian J 2010 *Phys. Rev. B* **82** 104521
- [12] Pfleiderer C 2009 *Rev. Mod. Phys.* **81** 1551
- [13] Schrieffer J R, Wen X G and Zhang S C 1989 *Phys. Rev. B* **39** 11663
- [14] Berk N F and Schrieffer J R 1966 *Phys. Rev. Lett.* **17** 433
- [15] Scalapino D J, Loh E and Hirsch J E 1986 *Phys. Rev. B* **34** 8190
- [16] Schrieffer J R 1995 *J. Low Temp. Phys.* **99** 397
- [17] Chubukov A V and Morr D K 1997 *Phys. Rep.* **288** 355
- [18] Frenkel D M and Hanke W 1990 *Phys. Rev. B* **42** 6711
- [19] Shraiman B I and Siggia E D 1992 *Phys. Rev. B* **46** 8305
- [20] Lüscher A, Milstein A I and Sushkov O P 2007 *Phys. Rev. B* **75** 235120
- [21] Singh A, Tesanovic Z and Kim J H 1991 *Phys. Rev. B* **44** 7757
- [22] Maiti S, Korshunov M M, Maier T A, Hirschfeld P J and Chubukov A V 2011 *Phys. Rev. Lett.* **107** 147002
- [23] Tanaka K et al 2006 *Science* **314** 1910  
Vishik I M et al 2012 *Proc. Natl Acad. Sci.* **109** 18332  
Ino A, Kim C, Nakamura M, Yoshida T, Mizokawa T, Shen Z-X, Fujimori A, Kakeshita T, Eisaki H and Uchida S 2000 *Phys. Rev. B* **62** 4137  
Razzoli E, Drachuck G, Keren A, Radovic M, Plumb N C, Chang J, Huang Y-B, Ding H, Mesot J and Shi M 2013 *Phys. Rev. Lett.* **110** 047004  
Peng Y et al 2013 *Nat. Commun.* **4** 2459
- [24] Psaltakis G C and Fenton E W 1983 *J. Phys. C: Solid State Phys.* **16** 3913
- [25] Lee H-J and Takimoto T 2012 *J. Phys. Soc. Japan* **81** 104704
- [26] Rowe W, Knolle J, Eremin I and Hirschfeld P J 2012 *Phys. Rev. B* **86** 134513
- [27] Chubukov A V and Musaelian K A 1995 *Phys. Rev. B* **51** 12605
- [28] Chubukov A V and Frenkel D M 1992 *Phys. Rev. B* **46** 11884
- [29] Kuchiev M Yu and Sushkov O P 1993 *Physica C* **218** 197  
Flambaum V V, Kuchiev M Yu and Sushkov O P 1994 *Physica C* **227** 267